JOURNAL OF GEOPHYSICAL RESEARCH, VOL. 104, NO. D17, PAGES 21,327–21,342, SEPTEMBER 20, 1999

Flux estimation of oceanic dimethyl sulfide around North America

S. Sharma,[1] L. A. Barrie,[1] D. Plummer,[2] J. C. McConnell,[2] P. C. Brickell,[1]
M. Levasseur,[3] M. Gosselin,[4] and T. S. Bates[5]

Abstract. Simultaneous measurements of atmospheric and surface water dimethyl sulfide (DMS) concentrations were taken aboard the icebreaker USCGC *Polar Sea* from July to October 1994, as part of a joint Canada/United States circumnavigation of North America, an expedition with a unique Arctic Ocean transect. Atmospheric DMS concentrations around North America varied between 0.25 and 50 nmol m^{-3} (mean = 5.1 nmol m^{-3}, σ = 8.5 nmol m^{-3}, n = 89) with highest values occurring near (south of) the Arctic ice edge. Surface water DMS concentrations ranged between 0.1 and 12.6 nmol L^{-1} (mean = 2.2 nmol L^{-1}, σ = 2.7 nmol L^{-1}, n = 46) with highest values in the western Arctic Ocean and off the U.S. east coast, near the Sargasso sea. In the Arctic Ocean, maximum concentrations in air and water were found along the ice edge in the Chukchi Sea region. Atmospheric DMS decay rates of 68% per day and 38% per day were deduced from observations between 70° and 76°N (continental shelf and slope of Chukchi Sea) on the west side and between 80° and 90°N (central Arctic Ocean) for the east side of the Arctic Ocean, respectively. Ocean to atmosphere flux estimates of DMS were determined using the Liss-Merlivat empirical dependence of exchange coefficient on wind speed, DMS air concentrations, Henry's law constants, and DMS water concentrations. DMS fluxes varied between 0.0017 and 30 μmol m^{-2} d^{-1}, respectively, with higher fluxes in regions with open water. The Arctic Ocean contributed 0.063 Tg S (DMS) (0.4% of DMS from the world oceans) during the summer of 1994. A simple one-dimensional (1-D) photochemical box model, applied to six case studies, showed that the atmospheric lifetime of DMS in the high Arctic was 2.5 to 8 days, whereas at 16°–33°N it was 1 to 2 days. Modeled DMS decay rates for these regions, using the 1-D model, accounted for only 33% of the measured decay rate. This result also suggests that halogen chemistry, reactions with Br/BrO, may be an important sink for DMS in the Arctic atmosphere.

1. Introduction

Dimethyl sulfide (DMS) is the dominant biogenic sulfur compound in the oceans [*Lovelock et al*., 1972; *Andreae et al*., 1986]. It is produced in the ocean and exchanged to the atmosphere where it reacts with OH radicals during daytime and NO_3 at night to form gaseous and particulate sulfur compounds. The oxidation mechanism involves both homogeneous and heterogeneous chemical reactions and produces sulfur dioxide (SO_2), sulfate (SO_4^{2-}), and methanesulfonic acid (MSA) [*Yin et al*., 1990; *Capaldo and Pandis*, 1997]. The resulting sulfate aerosol from DMS can contribute to acidification of the environment [*Charlson and Rodhe*, 1987] and aerosol radiative forcing of the climate system [*Charlson et al*., 1987; *Intergovernmental Panel on Climate Change* (*IPCC*), 1996]. The direct effect of sulfate aerosol on the radiative forcing has recently been estimated by *IPCC* [1996] to range between −0.21 and −0.8 W m^{-2} with a central value of −0.5 W m^{-2}.

From a global perspective, DMS emissions from the oceans contribute 15% to the total global sulfur annual emissions and about 50% to the natural sulfur emissions [*Bates et al*., 1992]. Most DMS observations have been carried out in midlatitude and low-latitude oceans including the sub–Arctic Ocean [*Bates et al*., 1987; *Ferek et al*., 1995]. Much less attention has been paid to the central Arctic Ocean [*Leck and Persson*, 1996]. In the Arctic environment during the summer, DMS emissions play an important role in influencing aerosol sulfate. During summer, biogenic sulfur sources contribute on average 30% of total sulfate at the baseline observatory at Alert (82.5°N), Canada [*Li and Barrie*, 1993]. Locally near ice edges where biological production is highest [*Wheeler et al*., 1996; *Gosselin et al*., 1999] this fraction will likely be much higher than 30%. Since aerosol number concentrations are often very low (10 to 100 cm^{-3}) (R. Leaitch et al., manuscript in preparation, 1999), cloud albedo in the north is particularly sensitive to changes in aerosol cloud condensation number concentration [*Twomey*, 1991; *Taylor and McHaffie*, 1994]. Thus it is important to assess the contribution of DMS emissions from the Arctic Ocean to the atmosphere.

In this paper, measurements of DMS concentrations in water and the atmosphere from the Arctic Ocean and around North America are reported. The data set includes the first observations across the Arctic Ocean. An atmospheric chemical transport model is used to predict atmospheric DMS con-

[1]Atmospheric Environment Services, Downsview, Ontario, Canada.
[2]Department of Earth and Space Science, York University, North York, Toronto, Ontario, Canada.
[3]Department of Fisheries and Oceans, Maurice Lamontagne Institute, Mont-Joli, Quebec, Canada.
[4]Department of Oceanography, University of Quebec, Rimouski, Quebec, Canada.
[5]Pacific Marine Environmental Laboratory, NOAA, Seattle, Washington.

Paper number 1999JD900207.
0148-0227/99/1999JD900207$09.00

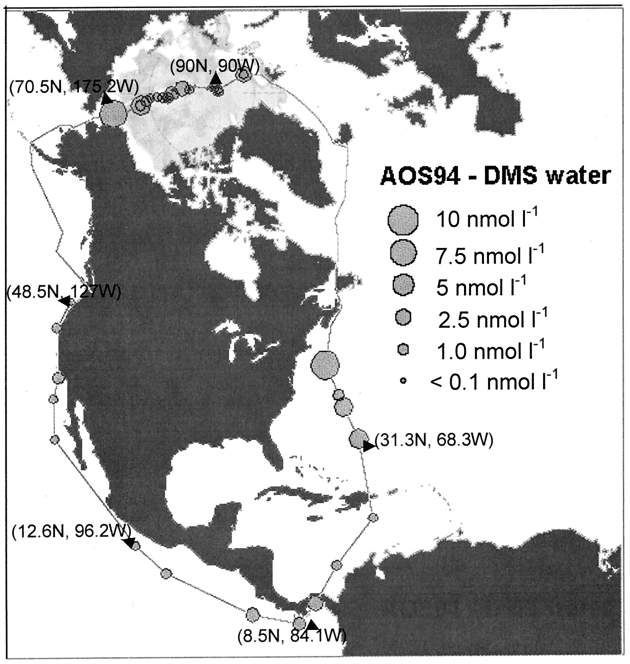

Figure 1. Surface water DMS concentrations along the ship's track during the AOS'94 expedition. The shaded area in the Arctic Ocean represents ice cover (frozen ocean surface) for August 1994. The ice edge was located around 70°N on the west side and 80°N on the east side of the Arctic Ocean.

centrations resulting from estimated DMS exchange between ocean and atmosphere and the oxidation of DMS.

2. Measurement Program

2.1. Study Area

Observations of atmospheric and seawater DMS were carried out aboard the USCGC *Polar Sea* from July 17 to October 5, 1994. The sampling areas covered different hydrographical regions of three oceans: Arctic, northwest Atlantic, and northeast Pacific as the ship circumnavigated North America and Greenland (Figure 1). After leaving Seattle, the ship traveled through the coastal waters of the northeast Pacific Ocean and entered the Arctic Ocean on the west via the Bering and Chukchi Seas (Plate 1). It then crossed the central Arctic Ocean via the North Pole exiting on the east side through the Fram Strait. It then traveled through the coastal and open regions of North Atlantic covering the Gulf of St. Lawrence, Sargasso Sea, and Caribbean Sea reaching the Pacific Ocean via Panama and eventually ending in Seattle.

2.2. Sampling and Analysis

Water samples for DMS analysis were collected at approximately 1 m depth with 12 L Niskin bottles attached to a rosette and at a depth of 5 m from the ship's uncontaminated water pumping system. These methods of collecting water DMS samples were compared several times on the ship and agreed within ±15%. Atmospheric DMS was collected from a height 20 m above sea level. These samples were preconcentrated on silanized glass tubes packed with Tenax-TA by a portable air sampler. Water temperature, wind speed, and direction were obtained from the ship's weather station for each sampling point.

A 5 mL water sample was transferred into a teflon chamber via a teflon loop and sparged immediately after collection with helium (ultrapure) at a rate of 65 mL min^{-1} for 5 min to remove 98% of the dissolved DMS [*Bates et al*., 1987]. The sparged gas was collected on silanized glass tubes packed with 170 ± 20 mg of Tenax-TA. The tubes were capped, sealed in teflon bags, and kept frozen until analysis. To avoid contamination from the ship's smokestack, atmospheric DMS samples were only collected when the ship was facing into the prevailing wind. Losses through the sampling system were minimized by using a portable sampler where a total volume of 2 L of air was pumped directly through the Tenax-TA tubes at a flow rate of 200 mL min^{-1} for 10 min. Upstream of the sample an oven-dried Whatman A/E type filter soaked in 5% KI/5% glycerol/0.5% Vitex (starch) was used to remove any oxidants from the sample stream. This oxidant scrubber has a long lifetime and turns color when exhausted [*Kittler et al*., 1992]. The tubes were preserved in a similar manner as the sparged water samples until analysis.

DMS concentrations were measured by a Hewlett Packard 5890 series II gas chromatograph equipped with a Sulphur Chemiluminescence Detector (SCD, Sievers Instruments Ltd.). Sample tubes were placed in the splitless injector of the GC and thermally desorbed at 170°C [*Sye and Wu*, 1992]. The experiments performed in the laboratory showed that 98% of DMS was recovered at this temperature. A sulfur specific SPB1 column (30 m, 4 μm thickness, 0.32 mm ID, Supelco Canada) was used to separate components at ambient temperature, and the signal was acquired by HP-Chemstation software through an HPIB board.

The system was calibrated by using two types of standards. For aqueous phase DMS a 3.7 nmol L^{-1} of working standard was prepared in 250 mL of distilled water. Five mL of this standard was sparged and analyzed in a similar manner as water samples. The atmospheric samples were standardized by transferring 50 μL of 2 mmol m^{-3} DMS gaseous standard (Scott Specialties) on Tenax-TA tubes and analyzed in a similar way to atmospheric samples. When equal weights of both standards were compared, the analysis was found to be within ±12% of each other. The limit of detection (defined as signal to noise ratio of 2:1) was 0.1 nmol L^{-1} for water samples and 6 pptv (0.25 nmol m^{-3}) for 2 L atmospheric samples. Accuracy and precision of the DMS measurement was ±12% [*Sharma*, 1997].

2.3. Sea to Air Flux Estimation

The calculation of the DMS flux from the ocean follows the same methodology as used by several other groups [*Andreae et al*., 1994; *Tarrason et al*., 1995; *Leck and Persson*, 1996; *Levasseur et al*., 1997]. The sea to air flux of DMS is a function of the surface turbulence and air-sea concentration gradient ΔC and is often parameterized as

$$\text{Flux} \uparrow = k_{\text{LM}} \times \Delta C = k_{\text{LM}}\left(C_w - \frac{C_a}{H}\right) \qquad (1)$$

where k_{LM} is the transfer velocity [*Liss and Merlivat*, 1986] which is a function of wind speed, temperature, and the diffusivity of DMS in water; C_w and C_a are the concentrations of DMS in the water and air, respectively; and H is the Henry's law coefficient, which is the ratio of concentrations of DMS in air to the dissolved concentration of DMS in water at equilibrium. In equation (1), C_a/H is usually negligible compared to

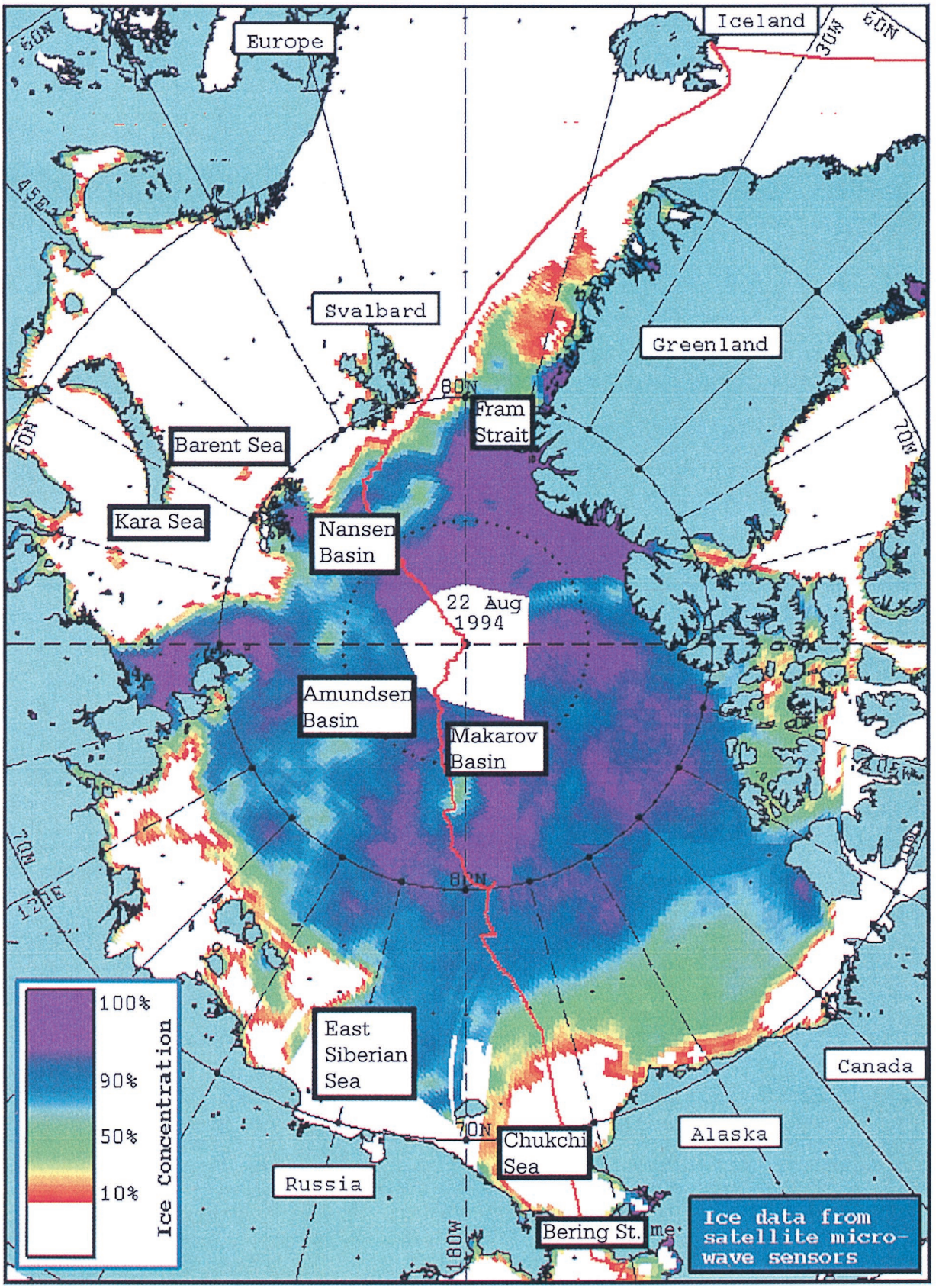

Plate 1. Sea-ice concentrations in different regions of the Arctic Ocean during the AOS'94 expedition. Sea-ice concentration data were not obtained for the sea-ice concentration near the North Pole.

C_w; ignoring C_a results in an overestimation of gas flux by less than 7% [*Leck and Rodhe*, 1991; *Levasseur et al*., 1997], and thus the flux of DMS is approximated as

$$\text{Flux} \uparrow = k_{\text{LM}} \times C_w \tag{2}$$

The wind speed dependence of k_{LM} has been determined by several investigators [*Liss and Merlivat*, 1986; *Smethie et al*., 1985; *Wanninkhof*, 1992; *Keeling et al*., 1998]. On average, transfer velocities calculated using Liss and Merlivat's wind speed-transfer velocity relationship are about 30% smaller than those derived from ^{222}Rn deficit techniques [*Smethie et al*., 1985; *Bates et al*., 1987] and 50% smaller than those calculated for CO_2 [*Wanninkhof*, 1992] and O_2 [*Keeling et al*., 1998]. This discrepancy may be due to application of results from small scale experiments which may not account for all of the processes controlling gas exchange to the vast areas of open ocean [*Wanninkhof*, 1992].

For the purpose of comparison with previous Arctic Ocean studies [*Leck and Persson*, 1996], we base our estimates of k_{LM} here on the transfer velocity-wind speed relationship of Liss and Merlivat. However, we note that our calculated fluxes may be low by a factor of 2. The wind speed-transfer velocity k_{LM} (cm h^{-1}) relationship of *Liss and Merlivat* [1986] is based on the three wind regimes as follows:

$$k_{\text{LM}} = 0.17uR^{0.65} \tag{3a}$$

$$\text{for } u \leq 3.6 \text{ m s}^{-1} \text{ (smooth regime)}$$

$$k_{\text{LM}} = (2.85u - 9.65)R^{0.5} \tag{3b}$$

$$\text{for } 3.6 < u \leq 13 \text{ m s}^{-1} \text{ (rough regime)}$$

$$k_{\text{LM}} = (5.90u - 49.3)R^{0.5} \tag{3c}$$

$$\text{for } u > 13 \text{ m s}^{-1} \text{ (wind-breaking regime)}$$

where u is the wind speed, R is the ratio of the Schmidt number of CO_2 at 20°C (660) to the Schmidt number of DMS at the surface seawater temperature ($\text{Sc}_{\text{CO2}}(20°\text{C})/\text{Sc}_{\text{DMS}}(T)$). Sc_{DMS} can be calculated from a temperature dependent third-order polynomial expression determined experimentally by *Saltzman et al*. [1993]:

$$\text{Sc}_{\text{DMS}}(T) = 2674.0 - 147.12T + 3.726T^2 - 0.038T^3 \tag{4}$$

where T is temperature in degrees Celsius.

The calculated flux of DMS to the atmosphere is also critically dependent upon the choice of wind fields. While the instantaneous flux can be best approximated using the local real-time wind, a regional or seasonal flux may be more realistic if based on the climatological wind speeds. For our instantaneous flux calculations we chose 6 hour averages of the observed wind speeds for a period centered on the time of observation. However, the climatological wind speeds were used for climatological fluxes.

Flux calculations for the Arctic Ocean over the ice pack are also complicated by the presence of ice [*Leck and Persson*, 1996]. The majority of uncertainty in the flux calculations comes from uncertainty in the flux equation. However, due to presence of ice there are other factors contributing to this uncertainty which can not be quantified. Below we discuss some of these factors:

1. There is a large uncertainty associated with our conversion of wind speeds from ship height of 30 to 10 m because the flux equations were derived with the observations at a height of 10 m. A neutral drag coefficient of 1.5×10^{-3} [*Liss and Merlivat*, 1986] was used for the open water, and 8×10^{-3} [*Guest and Davidson*, 1991] was used for frozen surfaces for these conversions.

2. Ignoring C_a only resulted in 7% overestimation which is small compared to uncertainties in other parameters of the flux equation.

3. It has been shown that gas exchange depends on the fetch of wind over water [*Wanninkoff*, 1992], that is, the distance traveled over water. Open leads can range anywhere from a few meters to several kilometers in dimension and could behave like different size lakes in a terrestrial terrain. In the absence of statistical data on lead size distribution, Leck assumed that the fetch was unlimited on the open water (open ocean conditions) for the eastern side of the Arctic Ocean (1996). It would be erroneous to apply such an assumption to the western Arctic Ocean due to more ice cover in this region than in the east. Transfer velocity was determined by applying ocean type conditions to a simulated lake type environment. In the model the area of open water was obtained, and fluxes were downscaled on the basis of percent open water in the Arctic Ocean. For other oceanic environments, unlimited fetch was assumed. The average calculated fluxes, both local and climatological, were downscaled by multiplying the estimated fluxes by the percentage of open leads for the specified latitude. There were two estimates used for the fraction of open water leads: first, data obtained from the ship observations which would give the flux estimate along ship's track for up to 3 km in radius around the sampling stations and second, the climatological fraction obtained from *Vowinkel and Orvig* [1970]. In the latter case, climatological wind speeds were used to estimate average fluxes for the Arctic Ocean and surrounding seas.

3. Measurements and Modeling (Results and Discussions)

3.1. Dimethyl Sulphide Concentrations

Observed DMS concentrations in water and air are shown in Figures 1 and 2 along the ship's track. The sampling stations were not equidistant, and individual measurements were taken as displayed by the symbol. For logistical reasons, DMS measurements in water did not begin until 70°N on the Pacific side.

For the entire expedition, DMS concentrations in water ranged from 0.1 to 12.6 nmol L^{-1} with a mean of 2.2 nmol L^{-1} ($n = 46$, $\sigma = 2.7$ nmol L^{-1}), while atmospheric DMS concentrations ranged from 0.25 to 50.8 nmol m^{-3} with a mean of 5 nmol m^{-3} ($n = 89$, $\sigma = 8.5$ nmol m^{-3}). In general, the lowest atmospheric concentrations corresponded to air arriving from oceanic regions with low algal productivity [*Wheeler et al*., 1996; *Gosselin et al*., 1999] or from the continent as shown by 5-day back trajectory analysis (Figure 3).

3.1.1. Surface water DMS: Arctic Ocean. During the Arctic Ocean transect, surface water DMS concentrations varied from less than 0.1 to 9.1 nmol L^{-1} with a mean of 2.0 nmol L^{-1} ($n = 27$) (Figure 1). The transect began at 70°N near the ice edge over a highly productive shelf region of the Chukchi Sea [*Wheeler et al*., 1996; *Gosselin et al*., 1999], where the highest water DMS concentrations were observed with a mean value of 5.08 ± 1.08 nmol L^{-1} (Table 1). This value is similar to the mean of 4.68 nmol L^{-1} obtained in the Bering Sea region during the spring bloom of 1981 [*Barnard et al*., 1984].

As the ship progressed through the less biologically productive regions of the Canada, Makarov, and Amundsen Basins [*Wheeler et al*., 1996; *Gosselin et al*., 1999], concentrations decreased to approximately 0.8 nmol L^{-1}. In surface water below the ice cover at the North Pole a DMS concentration of 1.2 nmol L^{-1} was observed which shows that in the presence of 100% ice cover there are still processes favoring the production of DMS in surface water [*Levasseur et al*., 1997]. Further support for this finding is the high concentration of 30 nmol L^{-1} DMS that was measured in ice just above the water-ice interface. During another icebreaker expedition to the North Pole in 1991 [*Leck and Persson*, 1996], an intensive study of the Fram Strait and Nansen Basin regions yielded a mean surface DMS value of 1.8 nmol L^{-1} which is close to the mean of 1.5 nmol L^{-1} for the same region observed in this study. Our surface water measurement of 1.2 nmol L^{-1} at the pole was a factor of 12 higher in August than the value of 0.1 nmol L^{-1} obtained by Leck's group in September. The difference in the concentrations measured between the two studies may be a result of the seasonal difference in microalgal productivity at the North Pole [*Leck and Persson*, 1996; *Gosselin et al*., 1999] or interannual differences in terms of mean water temperature, current, etc.

Detectable DMS concentrations in the range from 0.1 to 2.2 nmol L^{-1} were also found in 11 ice-surface melt ponds sampled. In summer of 1994 these ponds covered about 12% of the ice surface [*Perovich and Tucker*, 1999]. On a volumetric basis there was also 3 times as much DMS present in the bottom ice (ice located at 2–3 cm above the bottom of ice core) than at the water surface underneath the ice (M. Levasseur et al., manuscript in preparation, 1999). In spite of in situ production of DMS in the high latitudes, the atmospheric DMS exchange is limited to open leads, cracks in the ice cover, and the melt ponds.

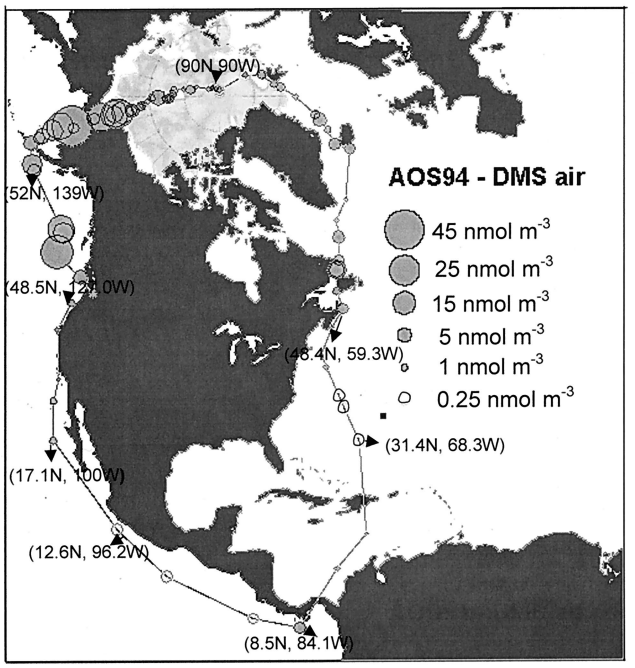

Figure 2. Atmospheric DMS concentrations along the ship's track during the AOS'94 expedition. The shaded area in the Arctic Ocean represents ice cover for August 1994. The ice edge was located around 70°N on the west side and 80°N on the east side of the Arctic Ocean.

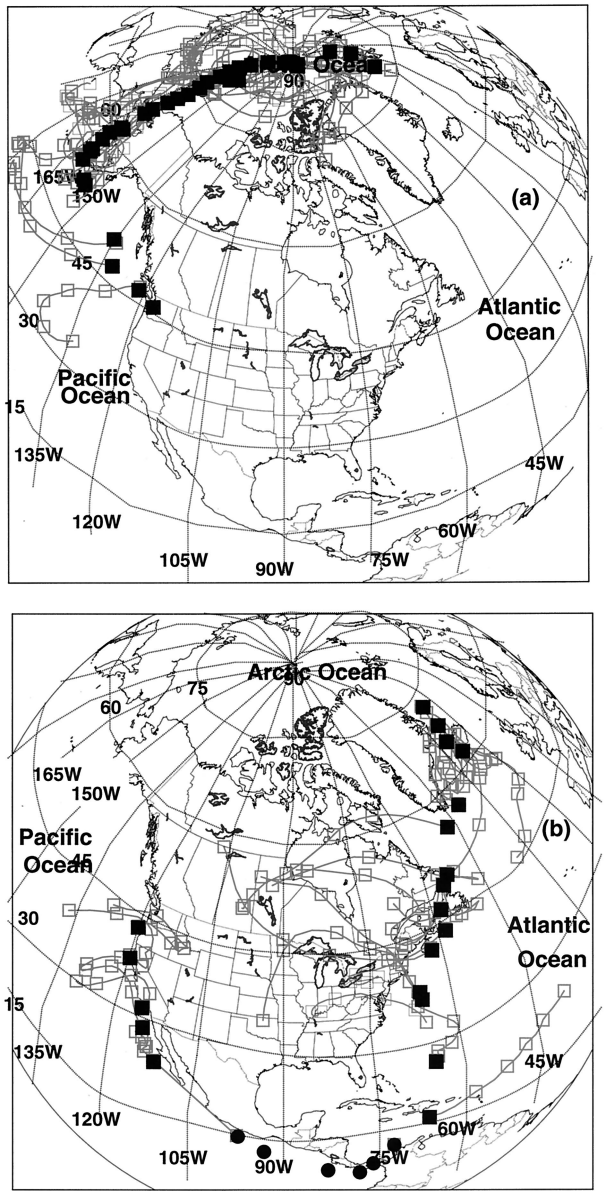

Figure 3. Five-day back trajectories (925 hPa) of air masses corresponding to atmospheric DMS concentrations as shown in Figure 2. (a) Trajectories from Seattle to the east side of the Arctic Ocean and (b) trajectories for the rest of the expedition. Solid square, sampling stations.

3.1.2. Surface water DMS: North Atlantic Ocean. In the coastal waters of the North Atlantic Ocean, water DMS concentrations ($n = 6$) varied from 12.6 nmol L^{-1} near the Gulf Stream to 5.1 nmol L^{-1} near the Sargasso Sea. High DMS concentrations observed in the North Atlantic may be a result of the fall bloom observed on the continental shelf and slope during September/October [*Parsons and Lalli*, 1988]. In September our observed average concentration of 7.7 nmol L^{-1} in the coastal region near the Sargasso Sea was 3.5 times (mean = 2.2 nmol L^{-1}) that observed by *Andreae et al*. [1985] during summer. As the ship progressed further into the Caribbean Sea, DMS concentrations decreased to 1.0 nmol L^{-1}. The variation found in the measured concentrations of water DMS was due to different productivity regions encountered along

Table 1. Flux Estimation (Mean and s.d.) of DMS Around North America From July to October 1994

Latitude and Month	Region	Average Observation C_w, nmol L^{-1}	$1-(C_wH^{-1}C_a^{-1})$, %	Wind Speed, m s^{-1}	k_{LM} Average, m d^{-1}	Sea Temperature, °C	Fraction Open Water, %	Extended Flux, μmol m^{-2} d^{-1} $(C_wk_{LM})_{avg}$
50°–70°N[a] July 18–27	Alaska coast (Bering Sea)	12.1	···	5.4	0.89	10.6	100	11.5
		(20.3)		(1.9)	(0.8)	(3.1)		(10.2)
70°–75°N July 27–31	Shelf and slope stations in Chukchi Sea	5.1	0.98	5.1	0.57	−1.43	25	0.73
		(1.9)		(2.3)	(0.2)	(0.1)		(0.15)
76°–80°N Aug. 1–9	Canada Basin	0.9	0.93	5.5	0.54	−1.53	3	0.007
		(0.5)		(2.0)	(0.4)	(0.2)		(0.011)
81°–90°N Aug. 9–22	Makarov and Amundsen Basin	0.8	0.95	7.2	0.97	−1.58	5	0.022
		(0.8)		(2.3)	(0.7)	(0.2)		(0.021)
84°–89°N Aug. 23–26	Nansen Basin	1.5	0.98	3.4	0.13	−1.62	6	0.012
		(1.1)		(1.6)	(0.4)	(0)		(0.13)
75°–90°N[b] Aug.	Fram Strait, Nansen Basin, Greenland Sea	2.3	0.97	6.0	0.83	−0.9	30	0.54
		(0.6)		(3.2)	(1.0)	(1.5)		(0.65)
50°–59°N[c] Sept. 5–7	Gulf of St. Lawrence	3.0	0.96	6.4	1.30	7.4	100	2.10
		(2.5)		(0.8)	(1.27)	(2.2)		(1.1)
26°–38°N Sept. 15–17	Coastal Atlantic Gulf Stream, near Sargasso Sea	7.7	0.99	4.0	0.51	26.3	100	2.7
		(4.5)		(1.1)	(0.29)	(3.1)		(3.6)
10°–16°N Sept. 19–21	Caribbean Sea	1.1	0.99	5.8	1.57	27.3	100	1.8
		(0.3)		(0.03)	(0.7)	(0.69)		(0.2)
6°–10°N Sept. 21–22	Gulf of Panama	2.4	0.99	4.6	0.97	26.7	100	2.8
		(0.3)		(0.9)	(0.6)	(0)		(1.2)
12°–45°N Sept. 23 to Oct. 5	Coastal Pacific regions	1.1	0.98	6.8	1.8	20.6	100	2.3
		(0.4)		(2.9)	(1.4)	(6.7)		(2.5)

Extended flux equal to flux times fraction open ocean.
[a]DMS_w taken from *Bates et al*. [1987].
[b]DMS_w taken from *Leck and Persson*, [1996].
[c]DMS_w taken from *Levasseur et al*. [1997].

the ship's track, although not measured, in the North Atlantic Ocean. The global primary production [*Longhurst et al*., 1995] in the coastal region was estimated from monthly mean chlorophyll fields (1979–1986) which were obtained by Nimbus 7 coastal zone color scanner (CZCS) radiometer. The variability found in different regions are as follows: Northeast Atlantic Continental Shelf (Gulf of St. Lawrence and Maine) equal to 1.48 g C m^{-2} d^{-1}, Canary Current Coastal (43°N–15°N) = 2.01 g C m^{-2} d^{-1}, and Central American Coastal equal to 0.92 g C m^{-2} d^{-1}, respectively.

3.1.3. Surface water DMS: North Pacific Ocean. Some variation was found in DMS concentrations in surface waters during the Pacific leg of the journey. Concentrations ranged from 0.66 to 1.84 nmol L^{-1} with a mean value of 1.1 nmol L^{-1} (σ = 0.4 nmol L^{-1}, n = 8). Similar concentrations were observed for the central and eastern North Pacific with a range of 1 to 2 nmol L^{-1} during vernal season by *Bates et al*. [1987]. In another study the concentration of DMS along the West Coast of the United States appeared to be seasonally dependent with a winter concentration of approximately 0.63 nmol L^{-1} as compared to the average summer concentration of 1.87 nmol L^{-1} for the upwelling season (May to August) [*Bates and Cline*, 1985]. In this study the mean DMS concentration was slightly lower probably due to our measurements being made after the upwelling season in October.

3.1.4. Atmospheric DMS: Arctic Ocean. Atmospheric DMS concentrations (Figure 2) were generally higher on the west side of the Arctic Ocean than on the east side varying from 14.7 nmol m^{-3} over the Alaskan Coast to 0.70 nmol m^{-3} over the Nansen Basin with a mean of 5.74 nmol m^{-3} for the entire Arctic Ocean transect. The highest DMS concentration was observed over the open waters of the Bering Sea, 880 km south of the ice edge on the west side of the Arctic Ocean. The concentration decreased drastically as the ship progressed into the ice pack and increased again as the ship exited the ice pack on the east side of the Arctic Ocean (Plate 1). This spatial difference in the data from ice edge to the ice pack is characteristic of algae growth on ice and its release from the ice as a result of melting of ice [*Fryxell and Kendrick*, 1988] and exchange with the atmosphere. One could argue that the decrease in concentration is primarily due to the physical and chemical dilution of atmospheric DMS as air parcels move away from the open water source regions onto the ice pack.

A detailed 5-day trajectory analysis was done around North America for all the sampling stations, (Figure 3) to obtain the origin of air masses in order to understand the spatial and temporal variability of the atmospheric DMS measurements. The back trajectory arriving at the 925 hPa level (Figure 3a) indicated air traveling from the Bering and Chukchi Seas regions onto the ice pack. Similar analysis done for the Greenland Sea/Fram Strait regions also indicated air arriving over the ice pack from the open ocean on the east side of the Arctic Ocean (Figure 3b). In the central Arctic region there was still measurable atmospheric DMS (1 nmol m^{-3}) which may be released by the larger open leads or breaks in the ice surface. The 5-day back trajectory analysis showed air masses encircling the central Arctic Ocean (Figure 3a) which may have scavenged fresh emissions from the local ocean sources.

Over the ice pack the question of how regionally representative are the measured DMS concentrations must be addressed. Are the DMS measurements indicative of the local sources or long range transport, or are they affected by the ship's ice breaking which could release trapped gases from underneath the ice cover? In order to assess the situation the following tests were performed. Two samples were taken, one at a height of 1 m above the freshly crushed sea ice and the

other at a height of 20 m above the ice cover. Concentrations obtained for the two samples were within sampling and analytical precision of 12%. If the ice breaking were contributing to atmospheric DMS, then we might expect some gradient in concentration at the two heights. For several samples we took our battery-operated portable sampler onto the ice pack several hundred meters away from the ship (source region) and found the same concentration of DMS as measured on board the ship at a height of 20 m. Thus the hypothesis that the ship affected atmospheric DMS concentrations in the vicinity of the ship was proven to be incorrect leading to the conclusion that observed DMS concentrations are representative of the ice pack.

Previously, atmospheric DMS concentrations in the Arctic have been measured only in two studies. One of the studies [*Ferek et al*., 1995] was carried out during the late spring/early summer (April to June) of 1991 and used ground- and aircraft-based DMS measurements on the west side of the Arctic Ocean at Barrow, Alaska. Maximum DMS concentrations were found during summer peaking at 4.6 nmol m^{-3} on one of the flights during late June at an altitude of 153 m, southwest of Barrow. During a flight north of Barrow to 74°N, concentrations of 0.9 nmol m^{-3} at a height of 153 m were obtained. This is half of the value of the mean DMS concentration that we observed at an altitude of 20 m in August for this region. The second study was conducted in the eastern part of the Arctic Ocean by Leck and Persson between August and October (International Arctic Ocean Expedition-91 (IAOE-91) [*Leck and Persson*, 1996]) with maximum DMS concentrations of 10 nmol m^{-3}, somewhat higher than our value of 6 nmol m^{-3}. The difference in the atmospheric DMS concentrations between the two studies was probably due to the variability of DMS concentrations in water which vary from year to year, the exchange process with the atmosphere, and the meteorological conditions.

3.1.5. Atmospheric DMS: North Atlantic Ocean. Similar trajectory analysis was also done for the North Atlantic Ocean. In the Denmark Strait on the east side of the Arctic Ocean the concentration of the atmospheric DMS varied between 1.5 and 6 nmol m^{-3}. Air parcels were from the Denmark Strait and the northwest Atlantic Ocean. In the Labrador Basin the concentration decreased to 0.67 nmol m^{-3} as the origin of air masses changed to the Hudson-Bay Lowland region of North America. In the Gulf of St. Lawrence region we observed concentrations as high as 11.1 nmol m^{-3} associated with trajectories originating in the Atlantic Ocean. The observed concentrations were consistent with those found by *Levasseur et al*. [1997] in August 1993 when the atmospheric levels of DMS varied from 0.5 nmol m^{-3} to 25 nmol m^{-3}.

As the ship moved through warmer regions of the North Atlantic (influenced by polluted air masses off the east coast of the United States) (Figure 3b), the concentration of DMS decreased to 0.25 nmol m^{-3}. The concentration increased to 5 nmol m^{-3} near the Gulf of Panama, but we could not obtain back trajectories for five sampling stations near the equator, so the origin of air for these stations is unknown.

Year-to-year variability in atmospheric DMS concentration was also seen in the comparison of these results with previous studies. The difference in results could have arisen from different meteorological parameters, location, or patchiness of the bloom during the 2 years. It could also be due to the scarcity of our data set in the North Atlantic as compared to other studies. The average concentration along the ship's track on the Atlantic side from 6.6°N to 58°N was 2.6 nmol m^{-3} (n = 7, σ = 3.2) in contrast to a winter average of 0.56 nmol m^{-3} (0.009–1.43 nmol m^{-3}) obtained for North and South Atlantic as far south as 58° during October to January [*Davison et al*., 1996]. During another study in the Atlantic Ocean in July near the east coast of United States from 25°N to 40°N, a mean value of 1.2 nmol m^{-3} was measured [*Cooper and Saltzman*, 1991].

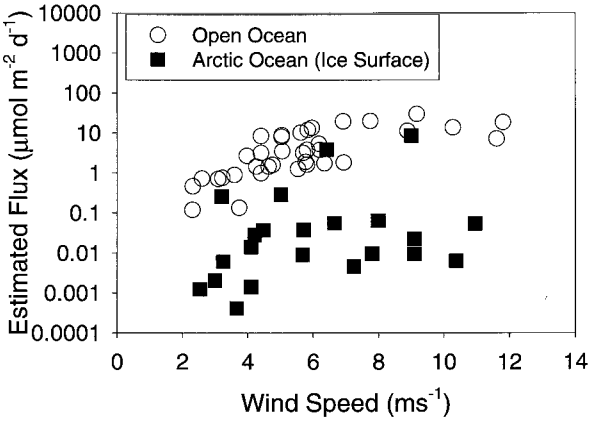

Figure 4. Estimated sea to air fluxes of DMS as a function of wind speed during the circumnavigation of North America, July to October 1994. Flux estimates in the Arctic were weighted by fraction open water area.

3.1.6. Atmospheric DMS: North Pacific Ocean. Off the western Canadian and Alaskan coast, atmospheric DMS concentrations during July ranged from 2 to 23 nmol m^{-3} with a mean of 12.7 nmol m^{-3} (n = 9, σ = 9.7 nmol m^{-3}). These were higher than the DMS concentrations that we observed off the West Coast of the United States in October which ranged from 0.25 and 1.74 nmol m^{-3} with a mean of 1.2 nmol m^{-3} (n = 9, σ = 0.6 nmol m^{-3}). In the North Pacific, air is mainly of marine origin in July (Figure 3b), whereas off the coast of California and Central America in October the 5 day back trajectories crossed regions of the coast and continent. Thus these results could have been influenced by different meteorological conditions (weather, season, location, wind speed).

3.2. Estimates of DMS Emissions

Table 1 shows DMS flux estimates on a latitudinal basis for different regions along the ship's track around North America. For the Alaskan coast and Fram Strait, average DMS concentrations were taken from other studies [*Bates et al*., 1987; *Leck and Persson*, 1996]. Wind speeds for these estimates were 6 hour averages (3 hours on either side of each sampling period). DMS fluxes for the entire expedition ranged from 0.0017 to 30 μmol m^{-2} d^{-1} (Figure 4) (x = 3.7 μmol m^{-2} d^{-1}, n = 68, and σ = 4.0). Wind speeds contributing to fluxes were between 2 and 12 m s^{-1}. The highest average flux of 11.5 μmol m^{-2} d^{-1} (n = 6, min = 10.2 μmol m^{-2} d^{-1}, σ = 6.1 μmol m^{-2} d^{-1}) was obtained for the Alaskan coast region between 65° to 70°N, and the lowest flux of 0.007 μmol m^{-2} d^{-1} (maximum equal to 0.1 μmol m^{-2} d^{-1}, n = 7) was in the Canada Basin between 76° to 80°N. Primary productivity was at a minimum in this region for the Arctic transect [*Wheeler et al*., 1996; *Gosselin et al*., 1999].

Fluxes were in good agreement with those from other studies. For the sub-Arctic region (50° to 70°N), *Bates et al*. [1987] estimated 13.1 μmol m^{-2} d^{-1}, while we estimated 11.3 μmol

Table 2. Average Sulfur (DMS) Emissions (1 s.d.) From the Arctic Marine Region, 65°–90°N in Summer (May to October) 1994

Region	Open Water $\times 10^{12}$ m^2 [a] (Percent Open of Total)[b]	Average DMS Flux for Arctic Ocean,[c] μmol m^{-2} d^{-1}	S Emission for August, Gg S	S Emission for Summer, Gg S
Bering Sea	0.8 (100%)	2.1 (1.7)	1.6	9.7
Greenland Sea	0.7 (21%)	2.1 (1.7)	1.4	8.5
Kara and Barent Seas	1.2 (35%)	2.1 (1.7)	2.4	14.5
Baffin Bay/Davis Strait	1.2 (100%)	2.1 (1.7)	2.4	14.5
Arctic Ocean (included Chukchi Sea)	0.4 (6%)	2.1 (1.7)	0.8	4.8
Melt Ponds (central Arctic Ocean)	0.84 (12%)	2.1 (1.7)	1.7	10.2
Canadian Archipelago	0.08 (11%)	2.1 (1.7)	0.2	0.97
Total S Emissions, Gg S			10.5	63.2

[a] *Parkinson and Cavalieri* [1989].
[b] *Vowinckel and Orvig* [1970].
[c] Average taken for Arctic Ocean and surrounding seas.

m^{-2} d^{-1} (n = 15, σ = 8.0 μmol m^{-2} d^{-1}). The only estimate made for the central Arctic Ocean (ice pack) by *Leck and Persson* [1996] was 0.024 μmol m^{-2} d^{-1} (σ = 0.034 μmol m^{-2} d^{-1}) in comparison to 0.041 μmol m^{-2} d^{-1} (n = 35, σ = 0.051 μmol m^{-2} d^{-1}) from this study. DMS flux estimates from the few observations in the North Atlantic in September yielded an average of 2.35 μmol m^{-2} d^{-1} (n = 9, σ = 0.47 μmol m^{-2} d^{-1}) compared to the estimate of *Tarrason et al.* [1995] of 1.95 μmol m^{-2} d^{-1} for summer. Finally, for the North Pacific we found 2.3 μmol m^{-2} d^{-1} (n = 9, σ = 2.5 μmol m^{-2} d^{-1}) compared to 2.4 μmol m^{-2} d^{-1} estimated by *Bates and Cline* [1985].

Tables 1 and 2 show estimates of sulfur (as DMS) emissions from the Arctic Ocean and surrounding seas. Open water areas for the different regions were obtained from *Parkinson and Cavalieri* [1989]. In Table 2 we used an average flux of 2.1 μmol m^{-2} d^{-1} obtained from the Arctic Ocean because concentrations from the surrounding seas were not available (taken from Table 1, averaging extended flux for 50°–90°N). Our results (Table 2) suggest that 10.5 Gg S and 63.2 Gg S were released by the Arctic Ocean for the month of August and the summer (May to October) of 1994, respectively.

DMS fluxes calculated by using climatological wind speeds were not significantly different from fluxes obtained by using instantaneous wind speed measurements over the Arctic Ocean. Observed average DMS water concentrations, climatological wind speeds, and water temperatures (Marine Climatic Atlas of the World, 1977) were used for climatological flux estimations from May through October. We estimate that the climatological fluxes for the Bering Strait and Chukchi Sea region were a factor of 3 higher than those for the central Arctic Ocean. Considering the area weighted mean for the two regions, a value of 2.1 μmol m^{-2} d^{-1} was obtained for the Arctic Ocean which is similar to the 2.0 μmol m^{-2} d^{-1} estimated by *Bates et al.* [1987] and *Leck and Persson* [1996]. If we assume constant water DMS concentrations, there is a factor of 2 uncertainty in this extrapolated value, obtained from 30% uncertainty in transfer velocity, 15% analytical uncertainty in DMS_w, 100% uncertainty in determination of percent open water for the Arctic Ocean, and finally 50% due to seasonal variation from May to October.

3.3. Reactivity of Atmospheric DMS: Case Studies

The DMS concentration in the atmospheric marine boundary layer (MBL) depends on its flux from the ocean, the rate of chemical removal, and the rate of mixing in the MBL. The main chemical losses are due to OH radicals (mainly during the daytime) and NO_3 radicals at night. [*Capaldo and Pandis*, 1997; *Yin et al.*, 1990]. OH levels depend on photolysis of O_3, H_2O mixing ratios, hydrocarbons, and NO_x levels, while NO_3 depends on O_3, ambient temperature, and NO_x levels in the marine boundary layer.

During the expedition around North America the highest concentration of atmospheric DMS was observed in the Bering and Chukchi Sea Arctic Ocean regions (Figure 2). The mean air temperature in this region was 2°C with an average wind speed of 7 m s^{-1}. Five day back trajectories indicate that air had passed over remote regions of the Arctic Ocean which were less influenced by the anthropogenic input. Thus NO_x levels (not measured) were likely low so that nighttime NO_3 removal was probably unimportant [*Heintz et al.*, 1996]. Likewise with lower temperatures, water concentrations were smaller so that OH levels were likely reduced below those at more tropical latitudes. We contrast this case with that of the Sargasso Sea with lower source strengths and different meteorological conditions. Atmospheric DMS concentrations in the Sargasso Sea were small or below the detection limit for the few measurements made. The reason for such low concentrations was probably due to lower fluxes (~4 times, see Table 1), warmer air temperature (27°C), and higher water vapor in the air (thus more OH). Also, the 5-day back trajectories indicate that the air masses had traveled for 3 days over the polluted east coast of the United States (no DMS over continent), giving higher NO_x and OH levels. These conditions would likely result in higher concentration of radicals with concomitant removal rates of DMS.

A decrease in atmospheric DMS concentrations was observed as the ship moved into the ice pack on the west side of the Arctic, and an increase was seen as the ship moved out of the ice pack on the east side. This was also noted by *Leck and Persson* [1996]. Figure 5a shows 5 day back trajectory analysis for observations corresponding to these situations. The trajectories were directed from open water region toward the ice pack for the west and east sides. The dependence of concentration on transport time over the ice (greater than 50% ice coverage) is shown in Figure 5b for the west and east sides. The figure shows a clear exponential decay with time. However, a steeper slope was obtained for the west side than for the east. For the west side of the Arctic the average decay in DMS was 68% per day, while it was 38% per day for the east side of the Arctic Ocean. In a similar study done in 1991 [*Leck and Persson*, 1996], an average decay of DMS of 35% per day was obtained for the east side of the Arctic Ocean. The difference in the slopes on west and east sides is likely due to two reasons. First, difference in the fractional ice coverage on the west and east (Plate 1) may have provided more ice surface on the west to facilitate the loss of gaseous DMS (physical or chemical). Second, the air masses on the west may be more polluted with precursors of OH and NO_3 radicals contributing to higher chemical dilution than the east.

A Lagrangian 1-D chemical model, developed by *Plummer et al*. [1996], was used to simulate this situation. Estimated DMS fluxes were the source of DMS for the model. The only atmospheric sinks were the oxidation reactions with OH and NO_3 radicals. Their concentrations were estimated on the basis of measured parameters such as the precursor concentrations of O_3 and volatile organic carbon (VOC). A brief description of this model is as follows.

The one-dimensional model used in this study is composed of 17 grid points, with variable spacing, stretching from the surface to a height of 1.85 km. Vertical mixing is performed

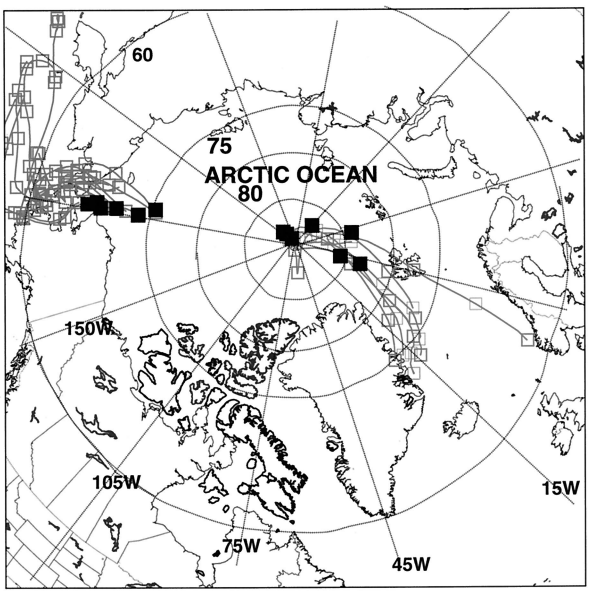

Figure 5a. Five day back trajectories corresponding to atmospheric DMS sampling times for sampling stations north of the ice edge as air masses move onto the ice pack traveling toward north from the west and east side of the Arctic Ocean. Solid square, sampling station. Ice edge (solid line) equal to 70°N on the west and 80°N on the east side of the Arctic Ocean.

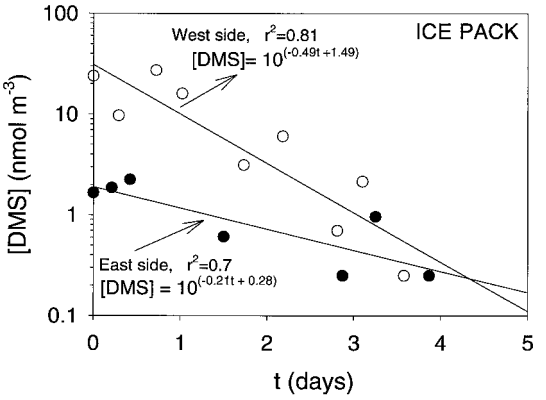

Figure 5b. Comparison of the atmospheric DMS concentrations as a function of transport time from ice edge (day 0) as air masses move onto the ice pack from the west and east side of the Arctic Ocean. Ice edge was 70°N on the west side and 80°N on the east side. Here t denotes travel time of air mass from ice edge in days.

using an eddy diffusion coefficient in the 1-D vertical transport equation. The eddy diffusion coefficient was kept constant at a value of 1.0×10^5 cm^2 s^{-1} over the bottom 450 m and set to a value of 1.0×10^3 cm^2 s^{-1} above. The vertical temperature gradient was dry adiabatic. Relative humidity was held constant at 75% for all runs.

The chemical mechanism does contain a full description of the important inorganic reactions as well as the oxidation of CO, methane, and ethane [*Plummer et al*., 1996]. Larger alkanes, alkenes, and aromatics are also included in the mechanism though these species have little effect on the chemistry for many of the runs. The initial oxidation reactions for DMS [*Koga and Tanaka*, 1993] with OH and NO_3 were added to the mechanism for this study. Subsequent reactions of the products were not included in the mechanism. OH and NO_3 were simulated since these are the important species for DMS lifetime. Photolysis rates are calculated at each time step accounting for ozone absorption, Rayleigh scattering, and surface reflectance by the method of *Yung* [1976]. Clouds were not considered in the calculation of the photolysis rates. Albedo was assumed to be 50% over ice surfaces [*Ebel et al*., 1990], 15% over land surfaces, and 5% over open water. Total column ozone amounts of 310 Dobson units (DU) were assumed for the Arctic and midlatitude cases, while a total ozone column of 260 DU was assumed for the trajectory ending in the Caribbean Sea.

Deposition velocities used were as follows: O_3 0.03 cm s^{-1} [*Lenshcow et al*., 1981; *Wesely et al*., 1981]; NO_2 0.02 cm s^{-1} [*Granat and Johansson*, 1983]; HNO_3 1.0 cm s^{-1}; H_2O_2 0.5 cm s^{-1}; aldehydes 0.75 cm s^{-1}; and PAN 0.06 cm s^{-1}. A constant NO flux of 1.2×10^8 molecules cm^{-2} s^{-1} was specified for all runs. Over a 500 m deep boundary layer this flux is equivalent to a NO production of 2400 molecules cm^{-3} s^{-1}.

This model was run along a trajectory from ice edge to ice pack along the longitude line from 70° to 76°N, along 170°W, on the west side and from 80° to 90°N, along 0°W (Greenwich Meridian) on the east side for 4 days. An initial concentration of 4.0 nmol m^{-3}. DMS was assumed in both cases, and water to air DMS fluxes, estimated from observations, were used as a source of atmospheric DMS. Model results in Figure 5c indicate a change in DMS with transport time over the ice

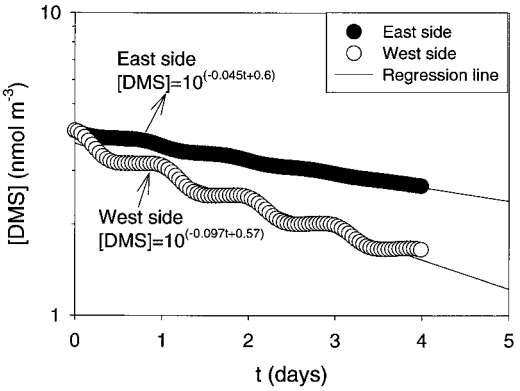

Figure 5c. Model-simulated atmospheric DMS concentrations for the west (70°–76°N, Chukchi Sea) and east (90°–80°N, central Arctic Ocean) for the two hypothetical trajectories (see text for details).

greater for the west than for the east. This is consistent with observations (Figure 5b). However, the predicted decay rate 2 (Figure 5c) was only 33% of that observed for the west and 23% of that observed for the east side (Figure 5b). Model-predicted decay was mainly due to OH radicals during the daytime (average [OH = 5.1×10^5 molecules cm^{-3}]). One source of uncertainty is the ability of our model to predict OH concentrations for the Arctic. In order to explain the observed decay rate of 67.6% in the western side of the Arctic, [OH] would have to be raised by a factor of 4 above our model-predicted rate to 2.1×10^6 molecules cm^{-3} (assuming an abstraction plus addition rate of reaction of OH with DMS of 6.3×10^{-12} molecules cm^{-3} s^{-1}). This is similar to the concentrations predicted by the model of *Prinn et al.* [1995], but chemical mechanisms of DMS oxidation in models are too uncertain in polar conditions [*Davis et al.*, 1998] for us to conclude that reactions other than those involving OH are responsible for the observed DMS decay. The inversion layer height was not measured, and was estimated (by using the wind speeds, temperature gradient, and atmospheric turbulence due to sea-wave amplitude) to be 500 m in agreement with the climatological Arctic inversion layer height [*Kahl*, 1990; *Kahl et al.*, 1992; *Serreze et al.*, 1992; *Nilsson*, 1996]. This might have introduced a decrease in concentration by 28% if the height was increased to 850 m (Table 4), but this is unlikely to be realistic over the frozen Arctic surfaces. This will be discussed later considering the results of sensitivity tests. Our model does not include the entrainment of air masses from free troposphere to the marine boundary layer. Dilution in the column as a result of this entrainment is about 35% if an entrainment rate of 0.6 cm s^{-1} is assumed [*Clarke et al.*, 1996]. However, this entrainment rate might be too fast for the more stable Arctic marine boundary layer and may not account for the discrepancy.

This 1-D model was also applied to the other six case studies (shown in Plate 2) in different marine environments. The purpose of this exercise was to predict the lifetimes of DMS in different marine environments. Six different trajectories were chosen and computed: (1) west side of the Arctic Ocean near ice edge, (2) central Arctic Ocean, (3) east side of the Arctic Ocean, (4) North Atlantic influenced by continental air masses, (5) cleaner North Atlantic, and (6) North Pacific off the coast of California. With the exception of cases 4 and 5 (locations marked on Plate 2), initial concentrations of O_3, CO, ethane, and propane were chosen to allow the final model concentrations to match the observations. For case 4, when the air mass is moving from North America out into the Atlantic, the model was run for 3 days over land with fluxes of hydrocarbons and NO_x representative of eastern North America. While over land, a diurnally varying boundary layer, with a maximum daytime depth of 1.4 km and minimum depth of 450 m, and deposition velocities for land were used. For the tropical Atlantic run (case 5) the initial O_3 concentration was set to 30 ppbv though due to photochemical destruction of O_3 within the model, the final concentration is much lower than that observed. Initial conditions for the six cases are given in Table 3. Mixing ratios of NO_x and O_3 were chosen on the basis of the region the trajectories pass through. The DMS flux used in the model was allowed to vary as the model moved along the trajectory. Initial DMS air concentrations for trajectories that originated above the boundary layer or over land (cases 3, 4, and 6) were set to zero. Initial DMS air concentrations for trajectories 1, 2, and 5 were set to 4.1 nmol m^{-3}, 1.2 nmol m^{-3}, and 1.2 nmol m^{-3}, respectively, the values representative of the source region. The flux into the model was variable at every step with latitude as given in Table 3.

The results of these six cases (Figure 6) indicate that the model-predicted DMS concentrations agreed well with observations within the bounds of uncertainty for reasonable initial concentrations and boundary conditions. To a large extent, uncertainties in the predicted DMS concentrations originate from uncertainties in the flux estimates. In case 1 the air mass passed over a region of high sea-to-air DMS fluxes, (Bering/Chukchi Sea), traveled over land for half a day, and then passed through different regions of varying DMS fluxes. Higher source regions contributed to higher measured DMS concentrations as confirmed by the modeled results. Case 2, representing the higher Arctic region, simulated an air trajectory circulating over Arctic frozen surfaces and showed a decay of DMS due to OH and NO_3 radicals in this region. Simulating case 2 with no DMS flux input gave similar results (14% difference) to simulation with DMS fluxes. In this case, three out of the five simulations had zero flux of DMS due to zero open ocean water (from observation up to 5 km) at that latitude. Thus this is a lower bound of the comparison for these extreme conditions. However, during the summer, 10% of the open water in the Arctic Ocean could contribute significant DMS to the atmosphere. Because of the longer lifetime of DMS in the Arctic atmosphere, even smaller contributions from the fluxes could be very important. For case 3, trajectories for two levels were coming from two different source regions. Thus we looked at the representativeness of 1000 hPa trajectory by comparing this trajectory with trajectories obtained from five other stations in the vicinity of the sampling station. Results indicated that 50% of the time the air masses were coming from Greenland, and the other 50% they were coming from the open ocean. Looking at the low DMS concentration measured at the sampling station, a 925 hPa trajectory was used in this case. Out of the 5 days in case 3, the air parcel traveled over Greenland for 3 days and over frozen surfaces of the Arctic Ocean for the other 2. The predicted DMS concentrations did not agree with the measured DMS within the bounds of uncertainty. The source region for this case was not certain as indicated by back trajectories and may have contributed to the discrepancy. In contrast to this, we also had a scenario in the warm Atlantic (case 4), when warm air traveled over land (polluted regions of North America) for 3 days and then over

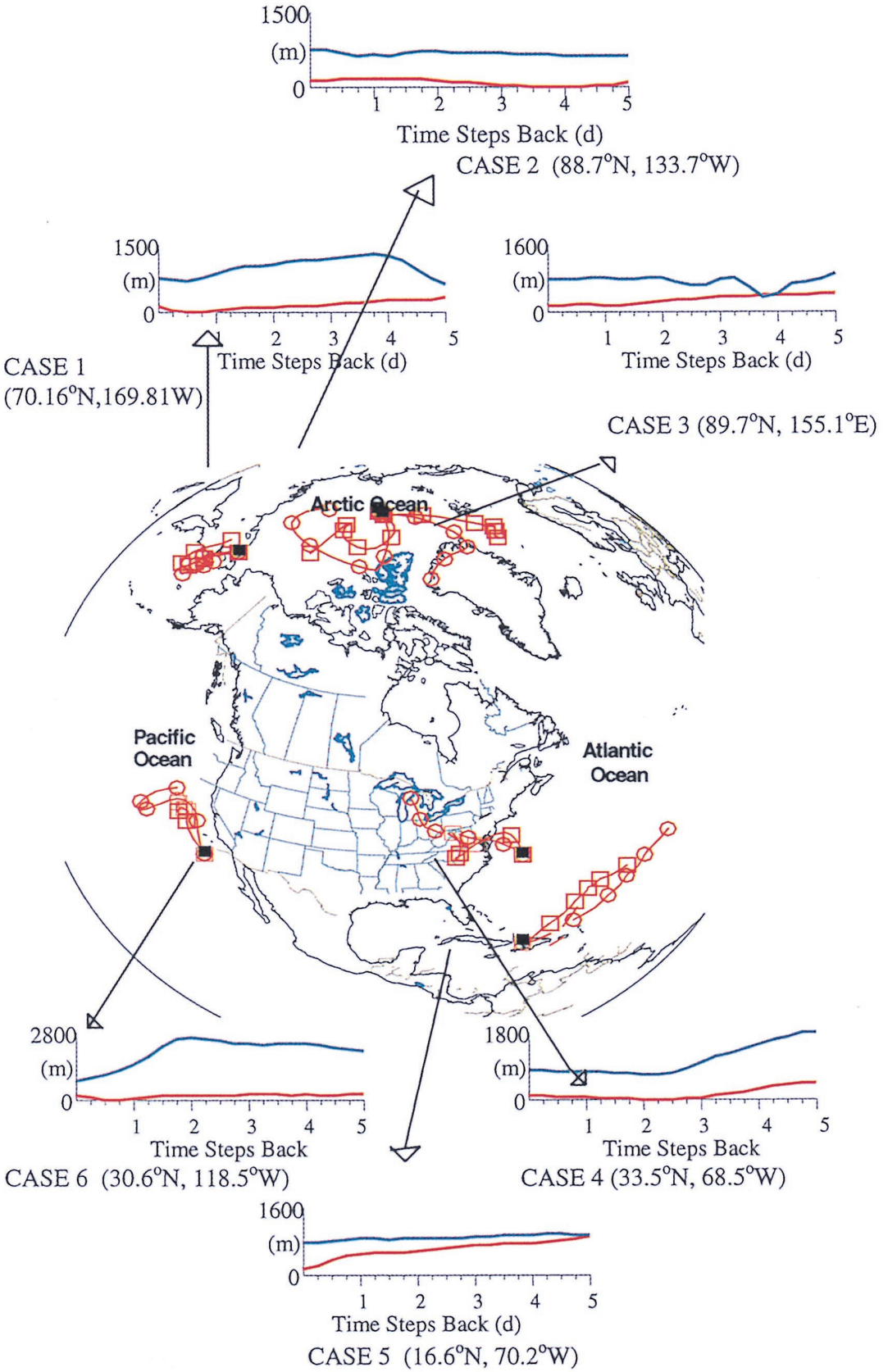

Plate 2. Back trajectory analysis (1000 and 925 hPa level) of six different cases chosen for model simulation of atmospheric DMS. Altitude plots of air masses for each case are shown, and zero time represents the sampling station. Solid square, sampling station; 1 time step equal to 1 day; open squares, 1000 hPa; open circles, 925 hPa pressure levels.

Table 3. Initial Conditions for the Six Case Studies as Shown in Figure 6

Case	NO_x, pptv	O_3, ppbv	CH_4, ppmv	CO, ppbv	C_2H_6, pptv	C_3H_8, pptv	ALKA, pptv	[DMS], pptv	DMS Flux, molecules cm^{-2} s^{-1}
1	30	30	1.83	115	780	80	50	100	8.3×10^9
									1.9×10^9
									7.2×10^9
									7.2×10^9
									7.2×10^9
									6.0×10^9
2	30	27	1.81	95	860	300	30	30	0
									2.7×10^7
									2.7×10^7
									2.7×10^7
									4.4×10^6
									3.2×10^6
3	30	30	1.81	100	760	300	30	0	0
									0
									1.3×10^9
									1.3×10^9
									1.8×10^8
									1.6×10^7
4	1000	75	1.81	200	1000	200	30	0	0
									0
									0
									5.8×10^9
									5.8×10^9
									6.9×10^9
5	30	30	1.83	95	500	120	10	30	3.2×10^8
									3.2×10^9
									1.1×10^9
									1.1×10^9
									1.1×10^9
									1.1×10^9
6	30	75	1.83	95	500	120	10	30	5.0×10^9
									9.3×10^7
									9.3×10^7
									9.3×10^7
									9.3×10^7
									1.2×10^9

Here pptv, parts per trillion by volume; ppbv, parts per billion; ppmv, parts per million.

a cooler ocean surface for the next 2 days. A more pronounced diurnal variability was seen in the model results in this case due to higher fluxes and large mixing ratios of OH and NO_3 calculated. Case 5 represented open-ocean conditions where air was over the warm North Atlantic for 5 days. A clear diurnal variability was also calculated for this case. Case 6, off the coast of California, showed air masses within the boundary layer for entire 5 days. The model-predicted concentration agreed very well with the measurements for this case. From these results it seems as if the model is not predicting well over the frozen Arctic surfaces as compared to open water. The source region for DMS over the frozen surfaces is defined by the percent open water. We have used these values from *Vowinkel and Orvig* [1970] and may not be providing accurate enough source strength for the model over the frozen surfaces.

For the six cases, lifetime of DMS was estimated for the losses due to OH radicals during the daytime and NO_3 during the night (Figure 7). Reasonable average mixing ratios of OH and NO_3 were produced by the model to obtain these lifetimes as shown in Table 4. In comparison to our results, the best estimate of spatial and temporal variation of OH and NO_3 mixing ratios were obtained by the Measurement of Ozone and Water Vapor by Airbus In-Service Aircraft (MOZART) model [*Brasseur et al*., 1998; *Hauglustaine et al*., 1998], which is a well accepted global atmospheric chemical and transport model. Our values for OH in all six cases differed by a minimum factor of 2 and maximum by a factor of 6, and NO_3 was different by a minimum factor of 2 and maximum by 20. The results indicate that the DMS had a long lifetime of 6–8 days in the central Arctic (88°N) under pristine conditions and a shorter lifetime of 0.75 day over the warm Atlantic Ocean in air masses influenced by the continental plume. Our results obtained are in reasonable agreement with those obtained elsewhere (measurements and model) (0.5 to 7 days) [*Berresheim*, 1987; *Barnes et al*., 1988; *Huebert et al*., 1993]. However, for the Arctic atmosphere, *Leck and Persson* [1996] has predicted a lifetime of 2.5 days for DMS. If such is the case, then considering our value of 8 days due to OH and NO_3 losses indicates that there are other removal processes for DMS such as halogen chemistry. Halogenated radicals such as bromine, chlorine, and their oxygenated forms may be involved in the DMS removal. However, the question is how much of these reactive halogen species is present in the Arctic atmosphere, and what are their respective rates of reactions with DMS? It has been hypothesized that the active component of gas phase bromine might be BrO radicals [*Hausmann and Platt*, 1994; *Miller et al*., 1997]. During the springtime, BrO is proposed to be important in tropospheric ozone depletion. Compared to average OH mixing ratios of 0.1 to 1 pptv, BrO has been measured as high as 17 pptv during the springtime [*Haussmann and Platt*, 1994].

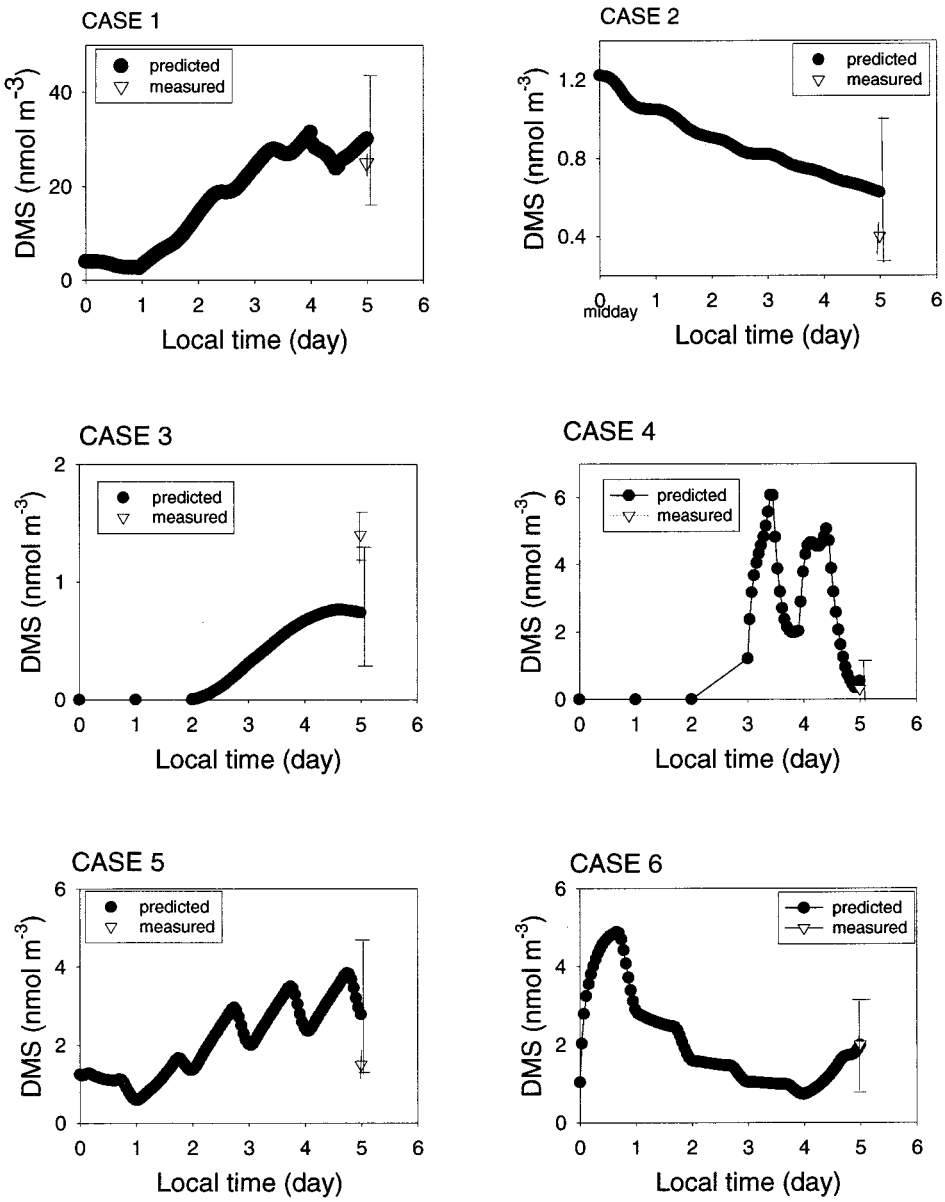

Figure 6. Model-predicted results of atmospheric DMS concentrations for six different oceanic environments during circumnavigation of North America. Estimated DMS is the most representative measurement in that region. The uncertainty (error bars) on the predicted DMS concentrations were obtained by using a 50% uncertainty in the estimated DMS fluxes. The initial conditions are given in Table 3.

However, during the summer under no ozone depletion conditions, the BrO mixing ratios are expected to be lower. The reaction rate of DMS with chlorine radicals, for example, is fast enough to make a significant difference [*Keene*, 1996]. Considering a mixing ratio of 0.5 pptv BrO [*Richter et al.*, 1998], the rates of reaction of OH radicals [*Barnes et al.*, 1988] with DMS is about a factor of 2 higher than that of BrO radicals [*Bedjanian et al.*, 1996]. Other model results [*Twomey*, 1994] have also suggested that BrO is an important sink for DMS during the daytime and could contribute as much as 24% (gas phase case) and 38% (aerosol/gas heterogeneous case) to DMS destruction. Thus DMS loss due to halogenated radicals could be of equal importance as OH chemistry.

Another speculation could be loss via possible heterogeneous reaction of DMS and ozone on the moist ice surface.

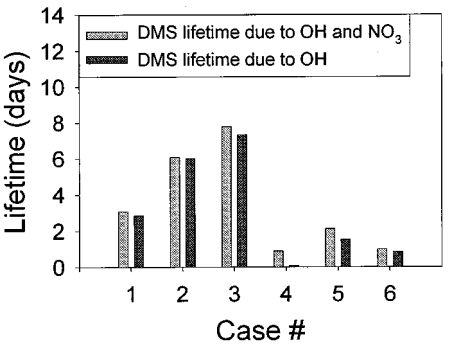

Figure 7. Lifetime of DMS obtained from the model simulation for the six different cases. Losses due to OH radicals during the daytime and NO_3 at night.

Table 4. Comparison of OH and NO_3 Radical Mixing Ratios as Generated by Our Model Calculations With Those of the MOZART Model

Case	Predicted OH,[a] pptv This Study	Predicted OH,[b] pptv MOZART	Predicted NO_3,[a] pptv This Study	Predicted NO_3,[b] pptv MOZART
1 (Aug.)	2.3×10^{-2}	0.84×10^{-2}	1.02×10^{-2}	3.67×10^{-2}
2 (Aug.)	1.2×10^{-2}	0.21×10^{-2}	0.08×10^{-2}	0.074×10^{-2}
3 (Aug.)	0.91×10^{-2}	0.16×10^{-2}	0.29×10^{-2}	0.08×10^{-2}
4 (Sept.)	0.08	0.14	4.29	2.25
5 (Sept.)	3.9×10^{-2}	4.2×10^{-2}	0.08	1.63
6 (Sept.)	7.3×10^{-2}	6.8×10^{-2}	0.09	0.89

The original modeled data were taken from MOZART [*Brasseur et al*., 1998; *Hauglustaine et al*., 1998], and results shown were taken from look-up table of chemical species in the Northern Aerosol Regional Climate Model (NARCM).

[a]Mixing ratios as predicted by our model.

[b]Mixing ratios as predicted by S. Gong et al. (personal communication, 1999).

There is plenty of open water and moist ice of similar ionic strength as fog water to facilitate such a reaction. The rate of reaction of DMS with ozone in aqueous phase is 4×10^8 M^{-1} s^{-1} [*Lee and Zhou*, 1994]. However, it is difficult to estimate the rate of this reaction on moist ice surface, and it would depend on deposition of both DMS and ozone to the surface before the reaction could take place.

A sensitivity test was also performed for this model. The purpose of this was to look at the effects of changing water albedo, height of mixed layer, and NO flux on the predicted DMS concentrations. Table 5 shows results obtained for such an analysis. The model was most sensitive to change in the mixing layer height and least sensitive to NO fluxes. A change of as much as 78% was observed by decreasing the boundary layer height to an unrealistic 250 m. In all of these runs an albedo of 5% was used for water, 15% was used for land, and 50% was used for ice surfaces. However, water albedo could vary by a factor of 2 around the ice edge. Thus, considering an albedo between 5 and 50%, a change of as much as −22.5% was observed in the predicted DMS concentration. Finally, an increase or decrease in NO flux by a factor of 2 changed DMS concentrations only by −7.8%. The predicted DMS concentrations were also not found to be sensitive to O_3 concentrations. The model is sensitive to initial DMS concentrations specifically in cases 2 and 5 where results could change if a different DMS concentration was used. Changes in OH radical concentrations (increase or decrease by a factor of 2) introduced a change of at most ±31% in the predicted DMS concentrations.

4. Summary and Conclusions

Three main goals were achieved in this study. First, the contribution of marine biogenic sulfur of 0.063 Tg was estimated for the summer months (May to October) from the Arctic Ocean and the surrounding seas. Although these emissions only contributed 0.4% to the global sulfur budget [*Bates et al*., 1992], these emissions are important on the regional basis and may affect cloud albedo during the summertime especially around the regions of the ice edge where highest DMS emissions were estimated. This was also supported by the back trajectory analysis indicating higher atmospheric DMS concentrations corresponding to regions of higher emissions.

Second, DMS emissions from the Arctic Ocean ice pack were lower and restricted to the open water leads than emissions near the ice edge and open water. A decline in atmospheric DMS concentrations of 68% per day was observed for the transport of DMS from the ice edge region to over the ice pack (70°–76°N) on the west side of the Arctic Ocean. But only 38% loss of DMS per day was obtained for 80°–90°N for the east side of the Arctic Ocean. These results are consistent with other studies. The difference in the loss rates could be related to conditions caused either by the chemistry or meteorology at the time of the measurements. However, DMS loss rates due to OH and NO_3 radicals were estimated with a 1-D photochemical model and were only 33% of the observed value. This indicates that additional DMS loss mechanisms are needed in our model such as those involving halogen chemistry (Br, Cl, and BrO radicals) which might have made a difference if included. Considering the BrO mixing ratios and rate of destruction of DMS by BrO, this loss mechanism could be of similar importance as OH chemistry.

Third, we have a better understanding of the large variation of atmospheric lifetimes of DMS in marine atmospheres from the tropics to the pole. The results indicated that DMS was longest-lived (8 days) in the Arctic and shortest-lived (0.8 day) in the warmer North Atlantic Ocean (near Sargasso Sea) due to OH and NO_3 radicals.

Our model has performed well within the bounds of uncer-

Table 5. Sensitivity Test for the One-Dimensional Lagrangian Model

Case Study	Water Albedo, %	Predicted [DMS], nmol m^{-3}	Δ, %	Planetary Boundary Layer, m	Predicted [DMS], nmol m^{-3}	Δ, %	NO Flux	Predicted [DMS], nmol m^{-3}	Δ, %
Case 1	2	36.9	0.3	250	65.5	78	↓ by x2	37.9	3
	5	36.8	···	500	36.8	···	no change	36.8	···
	10	35.7	−3	850	26.6	−28	↑ by x2	33.9	−7.8
	50	28.5	−22.5						

tainties. However, inclusion of halogen chemistry and possible heterogeneous reaction of DMS with ozone on moist ice surface may improve the model performance. There is also a need to establish rates of some of these reactions.

Acknowledgments. The authors would like to thank the following for their contributions toward this work: Atmospheric Environment Services (AES) for providing funding and support, NSERC and AES subvention for modeling work, Edna Templeton for her help in the model runs, Balbir Pabla for computing trajectories, John MacNeil for providing us with the trajectory plotting package, and Fred Hopper for starting the DMS program at AES. Finally, we would like to show our gratitude to Captain Bringham, his crew, and all the scientists on the Polar Sea for their support and help for making this possible.

References

Andreae, M. O., The ocean as a source of atmospheric sulfur compounds, in *The Role of Air-Sea Exchange in Geochemical Cycling*, edited by P. Buat-Menard, pp. 331–361, D. Reidel, Norwell, Mass., 1986.

Andreae, M. O., R. J. Ferek, F. Bermond, K. P. Byrd, R. T. Engstrom, S. Hardin, P. D. Houmere, F. LeMaurec, and H. Raemdonick, Dimethyl sulfide in the marine atmosphere, *J. Geophys. Res*., *90*, 12,891–12,900, 1985.

Andreae, T. W., M. O. Andreae, and G. Schebeske, Biogenic sulfur emissions and aerosols over the tropical South Atlantic, 1, Dimethylsulpfide in seawater and in the atmospheric boundary layer, *J. Geophys. Res*., *99*, 22,819–22,829, 1994.

Barnard, W. R., M. O. Andreae, and R. L. Iverson, Dimethyl sulfide and Phaeocystis poucheti in the southeastern Bering Sea, *Cont. Shelf Res*., *3*, 103–113, 1984.

Barnes, I., V. Bastian, and K. H. Becker, Kinetics and mechanisms of the reaction of OH with dimethyl sulfide, *Int. J. Chem. Kinet*., *20*, 415–431, 1988.

Bates, T. S., and J. D. Cline, The role of the ocean in a regional sulfur cycle, *J. Geophys. Res*., *90*, 9168–9172, 1985.

Bates, T. S., J. D. Cline, R. H. Gammon, and S. R. Kelly-Hansen, Regional and seasonal variations in the flux of oceanic dimethylsulfide to the atmosphere, *J. Geophys. Res*., *92*, 2930–2938, 1987.

Bates, T. S., B. K. Lamb, A. Guenther, J. Dignon, and R. E. Stoiber, Sulfur emissions to the atmosphere from natural sources, *J. Atmos. Chem*., *14*, 315–337, 1992.

Bates, T. S., K. C. Kelly, J. E. Johnson, and R. H. Gammon, A reevaluation of the open ocean source of methane to the atmosphere, *J. Geophys. Res*., *101*, 6953–6961, 1996.

Bedjanian, Y., G. Poulet, and G. Le Bras, Kinetics study of the reaction of BrO radicals with dimethylsulfide, *Int. J. Chem. Kinet*., *28*, 383–389, 1996.

Berresheim, H., Biogenic sulfur emissions from the subantarctic and Antarctic Oceans, *J. Geophys. Res*., *92*, 13,245–13,262, 1987.

Brasseur, G. P., D. A. Hauglustaine, S. Walters, P. J. Rasch, J. F. Muller, C. Granier, and X. X. Tie, MOZART, a global chemical transport model for ozone and related chemical tracers, 1, Model description, *J. Geophys. Res*., *103*, 28,265–28,290, 1998.

Capaldo, K. P., and S. N. Pandis, Dimethylsulfide chemistry in the remote marine atmosphere: Evaluation and sensitivity analysis of available mechanisms, *J. Geophys. Res*., *102*, 23,251–23,267, 1997.

Charlson, R. J., and H. Rodhe, Factors controlling the acidity of natural rain water, *Nature*, *295*, 683–685, 1987.

Charlson, R. J., J. E. Lovelock, M. O. Andreae, and S. G. Warren, Oceanic phytoplankton, atmospheric sulphur, cloud albedo and climate, *Nature*, *326*, 655–661, 1987.

Charlson, R. J., J. Langner, and H. Rodhe, Sulfate aerosol and climate, *Nature*, *348*, 22, 1990.

Clarke, A. D., T. Uehara, and J. N. Porter, Lagrangian evolution of an aerosol column during the Atlantic Startocumulus Transition Experiment, *J. Geophys. Res*., *101*, 4351–4362, 1996.

Cooper, D. J., and E. S. Saltzman, Measurements of atmospheric dimethylsulfide and carbon disulfide in the western Atlantic boundary layer, *J. Atmos. Chem*., *12*, 153–168, 1991.

Crutzen, P. J., and P. H. Zimmerman, The changing chemistry of the troposphere, *Tellus*, *Ser. AB*, *43*, 136–151, 1991.

Davis, D., G. Chen, P. Kasibhatla, A. Jefferson, D. Tanner, F. Eisele, D. Lenschow, W. Neff, and H. Berresheim, DMS oxidation in the Antarctic marine boundary layer: Comparison of model simulations and field observations of DMS, DMSO, $DMSO_2$, H_2SO_4(g), MSA(g), and MSA(p), *J. Geophys. Res*., *103*, 1657–1678, 1998.

Davison, B., et al., Dimethyl sulfide and its oxidation products in the atmosphere of the Atlantic and Southern Oceans, *Atmos. Environ*., *30*(10/11), 1895–1906, 1996.

Ebel, A., F. M. Neubauer, E. Raschke, and P. Speth, Surface albedo and global radiation over East-Asia from data of the geostationary satellite GMS, *Mitt. 72*, Inst. für Geophys. und Meteorol. der Univ. zu Köln, Köln, Germany, 1990.

Ferek, R. J., P. V. Hobbs, L. F. Radke, and J. A. Herring, Dimethyl sulfide in the arctic atmosphere, *J. Geophys. Res*., *100*, 26,093–26,104, 1995.

Fryxell, G. A., and G. A. Kendrick, Austral spring microalgae across the Weddell Sea ice edge: Spatial relationships found along a northward transect during AMERIEZ 83, *Deep Sea Res*., *Part A*, *35*, 1–20, 1988.

Gosselin, M., M. Levasseur, P. A. Wheeler, R. A. Horner, and B. C. Booth, New measurements of phytoplankton and ice algal production in the Arctic Ocean, *Deep Sea Res*., *Part II*, in press, 1999.

Granat, L., and C. Johansson, Dry deposition of SO_2 and NO_x in winter, *Atmos. Environ*., *17*, 191–192, 1983.

Guest, P. S., and K. L. Davidson, The aerodynamic roughness of different types of sea ice, *J. Geophys. Res*., *96*, 4709–4721, 1991.

Hauglustaine, D. A., G. P. Brasseur, S. Walters, P. J. Rasch, J. F. Muller, L. K. Emmons, and M. A. Carroll, MOZART, a global chemical transport model for ozone and related chemical tracers, 2, Model results and evaluation, *J. Geophys. Res*., *103*, 28,291–28,337, 1998.

Hausmann, M., and U. Platt, Spectroscopic measurement of bromine oxide and ozone in the high Arctic during Polar Sunrise Experiment 1992, *J. Geophys. Res*., *99*, 25,399–25,414, 1994.

Heintz, G., U. Platt, H. Flentje, and R. Dubios, Long-term observation of nitrate radicals at the Tor station, Kap Arkona (Riigen), *J. Geophys. Res*., *101*, 22,891–22,910, 1996.

Huebert, B. J., S. Howell, P. Laj, J. E. Johnson, T. S. Bates, P. K. Quinn, V. Yegorov, A. D. Clarke, and J. N. Porter, Observations of the atmospheric sulfur cycle on SAGA 3, *J. Geophys. Res*., 16,985–16,995, 1993.

Intergovernmental Panel on Climate Change (IPCC), *Climate Change 1995, The Science of Climate Change, Contribution of Working Group I to the Second Assessment Report of the Intergovernmental Panel on Climate Change*, edited by J. T. Houghton, L. G. Meira Filho, B. A. Callander, N. Harris, A. Kattenberg, and K. Maskell, Cambridge Univ. Press, New York, 1996.

Kahl, J. D., Characteristics of the low-level temperature inversion along the Alaskan Arctic coast, *Int. J. Clim*., *10*, 537–548, 1990.

Kahl, J. D., M. C. Serreze, and R. C. Schenell, *Atmos. Ocean*, *30*(4), 511–529, 1992.

Keeling, R. F., B. B. Stephes, R. G. Najjar, S. C. Doney, D. Archer, and M. Heimann, Seasonal variations in the atmospheric O_2/N_2 ration in relation to the air-sea exchange of O_2, *Global Biogeochem. Cycles*, *12*, 141–163, 1998.

Keene, W. C., Reactive chlorine: A potential sink for dimethylsulfide and hydrocarbons in the marine boundary layer, *Atmos. Environ*., *30*(6), 1–3, 1996.

Kittler, P., H. Swan, and J. Ivey, Technical note: An indicating oxidant scrubber for the measurement of atmospheric dimethylsulphide, *Atmos. Environ*., *Part A*, *26*(14), 2661–2664, 1992.

Koga, S., and H. Tanaka, Numerical study of the oxidation process of dimethylsulphide in the marine atmosphere, *J. Atmos. Chem*., *17*, 201–228, 1993.

Krol, M., P. J. van Leeuwen, and J. Lelieveld, Global OH trend inferred from methyl chloroform measurements, *J. Geophys. Res*., *103*, 10,697–10,711, 1998.

Leck, C., and C. Persson, The central Arctic Ocean as a source of dimethylsulphide seasonal variability in relation to biological activity, *Tellus*, *Ser. B*, *48*, 156–177, 1996.

Leck, C., and H. Rodhe, Emissions of marine biogenic sulfur to the atmosphere of northern Europe, *J. Atmos. Chem*., *12*, 63–86, 1991.

Lee, Y. N., and X. Zhou, Aqueous reaction kinetics of ozone dimethysulfide and its atmospheric implications, *J. Geophys. Res*., *99*, 3597–3605, 1994.

Lenshcow, D. H., R. Pearson, and B. B. Stankov, Estimating the ozone budget in the boundary layer by use of aircraft measurements of

ozone eddy flux and mean concentration, *J. Geophys. Res*., *86*, 7291–7297, 1981.

Levasseur, M., S. Sharma, G. Cantin, S. Michaud, M. Gosselin, and L. A. Barrie, Biogenic sulfur emissions from the Gulf of St. Lawrence and assessment of its impact on the Canadian East Coast, *J. Geophys. Res*., *102*, 28,025–28,039, 1997.

Li, S. M., and L. A. Barrie, Biogenic sulfur aerosol in the Arctic troposphere, 1, Contributions to total sulphate, *J. Geophys. Res*., *98*, 20,613–20,622, 1993.

Liss, P. S., and L. Merlivat, Air-sea exchange rates: Introduction and synthesis, in *The Role of Air-Sea Exchange in Geochemical Cycling*, edited by P. Buat-Menard, pp. 113–127, D. Reidel, Norwell, Mass., 1986.

Longhurst, A., S. Sathyendranath, T. Platt, and C. Caverhill, An estimate of global primary production in the ocean from satellite ratiometer data, *J. Plankton Res*., *17*(6), 1245–1271, 1995.

Lovelock, J. E., R. J. Maggs, and R. A. Rasmussen, Atmospheric dimethylsulfide and the natural sulfur cycle, *Nature*, *237*, 452–453, 1972.

Miller, H. L., A. Weaver, R. W. Sanders, K. Arpag, and S. Solomon, Measurements of arctic sunrise surface ozone depletion events at Kangerlussuaq, Greenland (67°N, 51°W), *Tellus*, *Ser. B*, *49*, 496–509, 1997.

Mitchell, J. F. B., T. C. Johns, J. M. Gregory, and S. F. B. Tett, Climate response to increasing levels of greenhouse gases and sulphate aerosols, *Nature*, *376*, 501–504, 1995.

Muller, J.-F., and G. P. Brasseur, IMAGES: A Three-dimensional chemical model of the global troposphere, *J. Geophys. Res*., *100*, 16,445–16,490, 1995.

Nilsson, E. D., Planetary boundary layer structure and air mass transport during the International Arctic Ocean Expedition 1991, *Tellus, Ser. B, 48*, 178–196, 1996.

Parkinson, C. L., and D. J. Cavalieri, Arctic sea ice 1973–1987: Seasonal, regional, and interannual variability, *J. Geophys. Res*., *94*, 14,499–14,523, 1989.

Parsons, T. R., and C. M. Lalli, Comparative oceanic ecology of the plankton communities of the subarctic Atlantic and Pacific Oceans, *Oceanogr. Mar. Biol. Annu. Rev*., *26*, 317–359, 1988.

Plummer, D. A., J. C. McConnell, P. B. Shepson, D. R. Hastie, and H. Niki, Modeling of O_3 formation at a rural site in S. Ontario, *Atmos. Environ*., *30*(12), 2195–2217, 1996.

Prinn, R. G., R. F. Weiss, B. R. Miller, J. Huang, F. N. Alya, D. M. Cunnold, P. J. Fraser, D. E. Hartley, and P. G. Simmonds, Atmospheric trends and lifetime of CH_3CCl_3 and global OH concentrations, *Science*, *269*, 187–190, 1995.

Richter, A., G. Wittrock, M. Eisinger, and J. P. Burrows, GOME observations of tropospheric BrO in northern hemispheric spring and summer 1997, *Geophys. Res. Lett*., *25*, 2683–2686, 1998.

Saltzman, E. S., D. B. King, K. Holmen, and C. Leck, Experimental determination of the diffusion coefficient of dimethylsulfide in water, *J. Geophys. Res*., *98*, 16,481–16,486, 1993.

Serreze, M. C., J. D. Kahl, and R. C. Schnell, Low-level temperature inversions of the Eurasian Arctic and comparisons with Soviet drifting station data, *J. Clim*., *5*(6), 616–629, 1992.

Sharma, S., Fluxes of dimethyl sulphide from the lakes of the Canadian Boreal Shield to the atmosphere, M.Sc. thesis, York Univ., Toronto, Ont., Canada, 1997.

Smethie, W. M., Jr., T. Takahashi, D. W. Chipman, and J. R. Ledwell, Gas exchange and CO_2 flux in the tropical Atlantic Ocean determined from ^{222}Rn and pCO_2 measurements, *J. Geophys. Res*., *90*, 7005–7022, 1985.

Sye, W.-F., and C.-Y. Wu, Advanced methodologies for adsorption/thermal desorption with Tenax-TA for the analysis of polycyclic aromatic hydrocarbons and sulfur compounds, *J. Chin. Chem. Soc*., *39*, 129–135, 1992.

Tarrason, L., S. Turner, and L. Floisand, Estimation of seasonal dimethyl sulphide fluxes over the North Atlantic Ocean and their contribution to European pollution levels, *J. Geophys. Res*., *100*, 11,623–11,639, 1995.

Taylor, J. P., and A. McHaffie, Measurements of cloud susceptibility, *J. Atmos. Sci*., *51*, 1298–1306, 1994.

Twomey, R., Aerosols, clouds and radiation, *Atmos. Environ*., *Part A*, *25*, 2435–2442, 1991.

Twomey, R., BrO as a sink for dimethylsulfide in the marine atmosphere, *Geophys. Res. Lett*., *21*, 117–120, 1994.

Vowinckel, E., and S. Orvig, *Climate of the North Polar Basin World Survey of Climatology*, Elsevier Sci., New York, 1970.

Wanninkhof, R., Relationship between wind speed and gas exchange over the ocean, *J. Geophys. Res*., *97*, 7373–7381, 1992.

Wesley, M. L., D. R. Cook, and R. M. Williams, Field measurements of small ozone fluxes to snow, wet bare soil and lake water, *Boundary Layer Meteorol*., *20*, 459–471, 1981.

Wheeler, P. A., M. Gosselin, E. Sherr, D. Thibault, D. Kirchman, R. Benner, and T. E. Whitledge, Active cycling of organic carbon in the central Arctic Ocean, *Nature*, *380*, 697–699, 1996.

Yin, F., D. Grosjean, and J. H. Seinfeld, Photooxidation of dimethyls sulfide and dimethyl disulfide, I, Mechanism development, *J. Atmos. Chem*., *11*, 309–364, 1990.

Yung, Y. I., A numerical method for calculating the mean intensity in an inhomogeneous Rayleigh scattering atmospher, *J. Quant. Spectrosc. Radiat. Transfer*, *16*, 755–761, 1976.

L. A. Barrie, P. C. Brickell, and S. Sharma, Atmospheric Environment Services, 4905 Dufferin Street, Downsview, Ontario, Canada M3H 5T4. (sangeeta.sharma@ec.gc.ca)

T. S. Bates and M. Gosselin, Department of Oceanography, University of Quebec, 300 Alle de Ursulines, Rimouski, Quebec, Canada G5L 3A1.

M. Levasseur, Department of Fisheries and Oceans, Maurice Lamontagne Institute, C. P. 1000, Mont-Joli, Quebec, Canada G5H 3Z4.

J. C. McConnell and D. Plummer, Department of Earth and Space Sciences, York University, 4700 Keele St., North York, Toronto, Ontario, Canada M3J 1P3.

(Received January 28, 1998; revised March 19, 1999;
accepted March 23, 1999.)